Stable Accumulation of Photosystem II Requires ONE-HELIX PROTEIN1 (OHP1) of the Light Harvesting-Like Family[1][OPEN]

Fumiyoshi Myouga,[a,2,3] Kaori Takahashi,[b] Ryoichi Tanaka,[b] Noriko Nagata,[c] Anett Z. Kiss,[d,e] Christiane Funk,[d,e] Yuko Nomura,[f] Hirofumi Nakagami,[f,4] Stefan Jansson,[d] and Kazuo Shinozaki[a,2,3]

[a]Gene Discovery Research Group, RIKEN Center for Sustainable Resource Science, Yokohama, Kanagawa 230-0045, Japan
[b]Institute of Low Temperature Science, Hokkaido University, Sapporo 060-0819, Japan
[c]Department of Chemical Biological Sciences, Japan Women's University, Bunkyo-ku, Tokyo 112-8681, Japan
[d]Umeå Plant Science Centre, Department of Plant Physiology, Umeå University, SE-901 87 Umea, Sweden
[e]Department of Chemistry, Umeå University, SE-901 87 Umea, Sweden
[f]Plant Proteomics Research Unit, RIKEN Center for Sustainable Resource Science, Yokohama, Kanagawa 230-0045, Japan

ORCID IDs: 0000-0003-0957-808X (F.M.); 0000-0002-5858-5326 (R.T.); 0000-0002-0894-2049 (N.N.); 0000-0001-5720-3325 (A.Z.K.); 0000-0003-2569-7062 (H.N.); 0000-0002-7906-6891 (S.J.); 0000-0002-6317-9867 (K.S.).

The cellular functions of two Arabidopsis (*Arabidopsis thaliana*) one-helix proteins, OHP1 and OHP2 (also named LIGHT-HARVESTING-LIKE2 [LIL2] and LIL6, respectively, because they have sequence similarity to light-harvesting chlorophyll *a*/*b*-binding proteins), remain unclear. Tagged null mutants of *OHP1* and *OHP2* (*ohp1* and *ohp2*) showed stunted growth with pale-green leaves on agar plates, and these mutants were unable to grow on soil. Leaf chlorophyll fluorescence and the composition of thylakoid membrane proteins revealed that *ohp1* deletion substantially affected photosystem II (PSII) core protein function and led to reduced levels of photosystem I core proteins; however, it did not affect LHC accumulation. Transgenic *ohp1* plants rescued with OHP1-HA or OHP1-Myc proteins developed a normal phenotype. Using these tagged OHP1 proteins in transgenic plants, we localized OHP1 to thylakoid membranes, where it formed protein complexes with both OHP2 and High Chlorophyll Fluorescence244 (HCF244). We also found PSII core proteins D1/D2, HCF136, and HCF173 and a few other plant-specific proteins associated with the OHP1/OHP2-HCF244 complex, suggesting that these complexes are early intermediates in PSII assembly. OHP1 interacted directly with HCF244 in the complex. Therefore, OHP1 and HCF244 play important roles in the stable accumulation of PSII.

Using the photosynthetic process, plants, algae, and photosynthetic bacteria capture solar energy in chemical forms that they and organisms at higher trophic levels use. Although photosynthesis is an incredibly complicated biochemical process, its molecular details have been analyzed precisely to an unparalleled level, down to the resolution of atomic structures and time resolutions of picoseconds. Nonetheless, the process is not understood completely, particularly the complicated nature of the biogenesis of PSII and its repair after damage caused by the excessive absorption of light energy. Many proteins assist in the multiple steps of PSII repair and assembly, in which assembly factors, such as chaperones, proteases, translocons, kinases, and phosphatases, have not yet been isolated or completely characterized (Lu, 2016).

Light absorption is the first step in the photosynthetic process. Detailed structures of the light-harvesting complexes (LHCs) of PSI and PSII have been elucidated in plants, algae, and cyanobacteria. Plant LHC proteins, which bind chlorophylls and carotenoids into a functional structure, consist of three membrane-spanning regions

[1] This work was supported by the RIKEN fund for plant science through grants to K.S. and F.M., Grants-in-Aid from the Ministry of Education, Culture, Sports, Science, and Technology Japan (Japan Society for the Promotion of Science; 24710219 to F.M.; 26650106 and 15H01247 to H.N.), the Young Researchers Overseas Visit Program of the Japan Society for the Promotion of Science to K.S. and F.M., the Swedish Research Council to S.J., and by the Swedish Energy Agency (2012-005889 to C.F.).

[2] These authors contributed equally to the article.

[3] Address correspondence to fumiyoshi.myouga@riken.jp or kazuo.shinozaki@riken.jp.

[4] Current address: Max Planck Institute for Plant Breeding Research, Carl-von-Linne-Weg 10, 50829 Cologne, Germany.

The author responsible for distribution of materials integral to the findings presented in this article in accordance with the policy described in the Instructions for Authors (www.plantphysiol.org) is: Kazuo Shinozaki (kazuo.shinozaki@riken.jp).

F.M., S.J., and K.S. designed the research; F.M., K.T., R.T., N.N., A.Z.K., Y.N., and H.N. conducted experiments; F.M., R.T., H.N., C.F., and S.J. analyzed the data; F.M. wrote the article with contributions from all other authors.

[OPEN] Articles can be viewed without a subscription.

www.plantphysiol.org/cgi/doi/10.1104/pp.17.01782

per polypeptide and are encoded by nuclear LHC genes (Liu et al., 2004; Standfuss et al., 2005). However, all organisms performing oxygenic photosynthesis also contain light-harvesting-like (Lil) proteins that are possibly involved in photoprotection instead of harvesting light energy (Jansson, 2005; Engelken et al., 2010; Neilson and Durnford, 2010).

Members of the large family of Lil proteins are regulated in a manner opposite to that of LHC proteins under high light intensity. Most *Lil* genes are up-regulated whereas the expression of *LHC* genes is repressed, suggesting important roles of Lil proteins in protection against stress caused by high light intensity (Klimmek et al., 2006). This group includes the early light-induced proteins ELIP1 and ELIP2 (also known as Lil1), which consist of three transmembrane helices. The stress-enhanced proteins SEP1 and SEP2 (also known as Lil4 and Lil5, respectively) and Lil3.1 and Lil3.2 proteins each contain two transmembrane helices, whereas the one-helix proteins OHP1 and OHP2 (also known as Lil2 and Lil6, respectively) contain only one transmembrane helix. The common structure in all members of the Lil family is the light-harvesting chlorophyll *a*/*b*-binding (CAB) domain, which is necessary for the pigment-binding properties of LHCs (Adamska et al., 1999; Funk, 2001; Storm et al., 2008; Staleva et al., 2015).

Lil proteins have been shown to function in direct protection of PSI and PSII, as shown for subunit S of PSII (PsbS; Niyogi et al., 2005), to regulate pigment biosynthesis (Xu et al., 2002; Rossini et al., 2006; Sobotka et al., 2008; Tanaka et al., 2010; Takahashi et al., 2014), and to function as pigment stabilizers, carriers, or both (Xu et al., 2002, 2004; Rossini et al., 2006; Yao et al., 2007, Hernandez-Prieto et al., 2011; Knoppová et al., 2014). However, despite the ubiquity and abundance of these proteins, the understanding of their precise functions at the molecular level in plants is limited (Casazza et al., 2005; Mishra et al., 2012).

The Arabidopsis (*Arabidopsis thaliana*) genome contains two OHP genes, *OHP1/Lil2* (At5g02120) and *OHP2/Lil6* (At1g34000). These genes encode proteins of 110 and 172 amino acids, respectively, with calculated molecular masses of about 12 to 19 kD. Moreover, increased expression of *OHP1* is observed under light stress (Jansson et al., 2000). The presence of the antisense gene *NDP1*, which partially overlaps the 3′ untranslated region of *OHP1*, also is reported (Stawski et al., 2014). However, no other studies of the functions of *OHP1* have been reported. OHP2 accumulates in PSI as light intensity increases and, therefore, is proposed to have a photoprotective function (Andersson et al., 2003). In cyanobacterium (*Synechocystis* sp. PCC 6803), five Lil proteins containing one transmembrane helix are present, called high-light-inducible proteins (Hlips; Dolganov et al., 1995) or small CAB-like proteins (Scps; Funk and Vermaas, 1999). It is anticipated that plant OHPs have similar functions to cyanobacterial Hlips/Scps (Engelken et al., 2010).

The putative short-chain dehydrogenase/reductase Ycf39 and two members of the Hlip/Scp family, HliC (ScpB) and HliD (ScpE), are associated with the reaction center II complex (Knoppová et al., 2014), and the chlorophyll synthase-HliD subcomplex is associated with the Ycf39 protein, or YidC/Alb3 insertase, or both (Chidgey et al., 2014). These results suggest that the Ycf39-HliD complex participates in the efficient assembly of PSII by stabilization of the newly synthesized D1 protein and replacement of photodamaged D1 during PSII repair. Moreover, HliD binds with chlorophyll *a* and β-carotene and dissipates absorbed energy via direct energy transfer from chlorophyll to the carotenoid (Staleva et al., 2015). Thus, a similar mechanism may be relevant for biosynthesis of the D1 protein and energy quenching in the plant LHC superfamily.

Our research group has been collecting transposon *Ds*- and T-DNA-tagged nuclear mutants for genes that encode chloroplast proteins and has been systematically analyzing their phenotypes to understand chloroplast functions. We have created the Chloroplast Function Database (Myouga et al., 2010, 2013) to share the resulting data (http://rarge-v2.psc.riken.jp/chloroplast/). Using our mutant collection, we have been precisely analyzing *albino and pale green* (*apg*) mutants to find an *apg* mutant (*apg16*) that could be used as a tagged mutant for *OHP1*. Here, we precisely analyzed the tagged *apg16/ohp1-1* mutant and other *OHP1* and *OHP2* mutants to identify how *OHP1* functions in the biogenesis and repair of PSII. We further identified that OHP1 associates not only with the minimal reaction center complex of PSII but also with proteins involved in the assembly of its core components.

RESULTS

Identification of Mutant Alleles of the One-Helix LHC-Like Proteins OHP1 and OHP2

We isolated the *apg16* mutant for the *OHP1* gene (At5g02120) in our Arabidopsis mutant collection of nucleus-encoded chloroplast proteins (Myouga et al., 2013). To identify the function of the 7.4-kD mature OHP1 protein, we isolated additional Arabidopsis T-DNA insertion mutants for *OHP1* and screened them for potential defects in growth and color under long-day conditions (a 16-h light period with a photosynthetic photon flux density of 75 μmol m^{-2} s^{-1}). Two T-DNA insertion alleles were obtained: one allele (*ohp1-1*) had a T-DNA insertion in the first exon of the coding region (+60 bp), while the other allele (*ohp1-2*) had a T-DNA insertion in the second exon (+182 bp; Fig. 1, A and B). They showed reduced growth and pale-green leaves compared with the wild type when grown on Murashige and Skoog medium (MSM) agar plates. Similarly, Arabidopsis T-DNA insertion mutants of a second one-helix LHC-like protein named OHP2 (*Lil6*; At1g34000; Andersson et al., 2003) produced seedlings with pale-green leaves and retarded growth on agar plates. We also isolated two alleles of *ohp2* mutants (Fig. 1, A and B) and used them as controls for comparison with the *ohp1* mutant phenotype. Following the transfer of homozygous *ohp1* and *ohp2* mutants to soil,

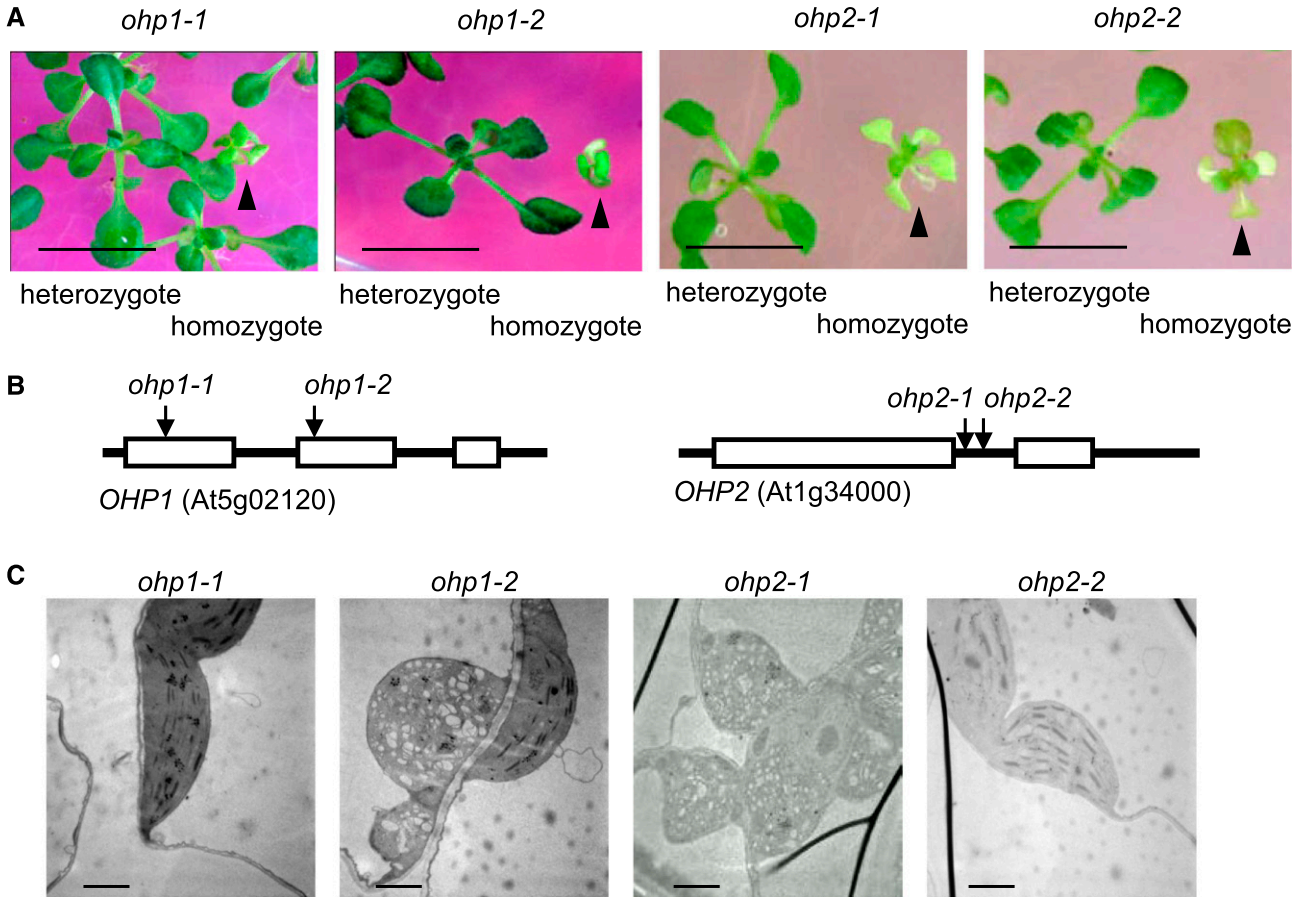

Figure 1. Phenotypic characterization of the *ohp1* and *ohp2* mutants. A, Four-week-old Arabidopsis seedlings on agar medium supplemented with 1% Suc: two *ohp1* mutants and two *ohp2* mutants (*ohp1-1* in the Landsberg *erecta* [L*er*] background, *ohp1-2* and *ohp2-2* in the Columbia background, and *ohp2-1* in the Wassilewskija background). Pale-green plants are homozygous (at right, indicated by arrowheads). Green seedlings are heterozygous (at left). Bars = 1 cm. B, Schematic representation of *OHP1* and *OHP2* gene structures. Boxes indicate exons, and lines indicate introns. Arrows indicate the positions of T-DNA insertions in the four mutant alleles. C, Transmission electron micrographs of plastids from homozygous mutants in *ohp1* and *ohp2* mutants. Bars = 2 μm.

all plants withered and died. The chloroplast ultrastructure in developing leaves of *ohp1* and *ohp2* mutants was investigated using transmission electron microscopy. Chloroplasts of wild-type plants had a characteristic lens-like shape and a well-developed thylakoid membrane system with numerous granal stacks (Supplemental Fig. S1). However, leaves of homozygous *ohp1* and *ohp2* mutants had fewer thylakoid membranes with granal stacks than those of wild-type plants (Fig. 1C), indicating that chloroplast development and differentiation had been affected. Reverse transcription PCR (RT-PCR) analysis showed that mRNA of *OHP1* was not detectable in *ohp1-1* and *ohp1-2* mutants (Supplemental Fig. S2C), indicating that both alleles are null mutations. Similar results also were obtained in two alleles of *ohp2* mutants (Supplemental Fig. S2C). To demonstrate that the phenotype of the *ohp1* mutants was attributable to mutation of the *OHP1* gene, we conducted complementation experiments with *ohp1* mutants as the background by inserting a 1.5-kb genomic fragment that contained a 1-kb *OHP1* promoter region and the 0.5-kb full-length *OHP1* gene sequence. Transgenic plants grew normally with full-green phenotypes, which indicated that growth defects were caused by T-DNA insertions in the *OHP1* gene of the *ohp1* mutants (Supplemental Fig. S2A). Moreover, a negative impact of OHP1 overexpression was not observed by transformation with *OHP1* cDNA driven by the cauliflower mosaic virus (CaMV) 35S promoter in wild-type plants (Supplemental Fig. S2B). Thus, *OHP1* and *OHP2* play an essential role in chloroplast development as well as in vegetative growth. The chlorophyll content (fresh weight basis) in the null mutants, when grown on an agar plate with 1% Suc, was approximately 40% of that in wild-type plants because of defective chloroplast development (Supplemental Fig. S2D).

Characterization of the *OHP1* Gene and Expression Analysis

OHP1 transcripts accumulated rapidly under high-light stress according to the results of RNA-blot analysis (Supplemental Fig. S3). We analyzed the expression of *OHP1* throughout the developmental stages of

Arabidopsis in more detail by examining tissue-specific staining patterns of transgenic plants carrying a specific *OHP1* promoter (*pOHP1*)::*GUS* fusion construct. We observed strong GUS staining of *pOHP1*::*GUS* transgenic Arabidopsis plants in seedling cotyledons and shoot apices in young and mature plants (Fig. 2A). Under high-light stress, GUS activity was strongly induced in all organs of young plants (Fig. 2A). The GUS staining pattern suggested that OHP1 functions mainly in the early stage of chloroplast development under normal growth conditions and that OHP1 production is induced in all vegetative tissues when they are exposed to stress caused by high light intensity.

OHP1 and OHP2 contain putative N-terminal chloroplast-targeting sequences. Both proteins contain single transmembrane domains in their amino acid sequences, which suggests that OHP1 and OHP2 are tightly attached to thylakoid membranes. To confirm the localization of these proteins in chloroplasts of plant cells, we created fused constructs of full-length *OHP1* and *OHP2* cDNAs with synthetic GFP (sGFP) at their C termini. sGFP fusion proteins were transiently produced in epidermal cells of tobacco (*Nicotiana tabacum* 'SR1') leaves by means of particle bombardment, and GFP fluorescence was observed in chloroplasts (Fig. 2B).

Chlorophyll Fluorescence Analysis Reveals Defects in PSII Function in *ohp1* Mutants

During the isolation of homozygotes from *ohp1-1* and *ohp1-2* mutants, we noticed that the mutants showed typical phenotypes related to stress caused by high light intensity, such as paler and whitish leaves. The mutants' stunted growth and sensitivity to high light levels suggested a possible defect in photosynthesis. To investigate the light sensitivity of these mutants, we measured chlorophyll fluorescence in leaves of 3-week-old whole plants (Supplemental Table S1). The F_v/F_m ratio was measured to determine maximum quantum yield, which represents an estimate of the maximum proportion of absorbed quanta used in PSII reaction centers (Kitajima and Butler, 1975). F_v/F_m decreased greatly in the *ohp1-1* mutant (0.53 in the *ohp1-1* mutant versus 0.85 in the wild type) at three different light intensities (Supplemental Table S1), suggesting that PSII experienced light damage or was misassembled even under low-light growth conditions. Damage to *ohp1-1* and *ohp1-2* mutants caused a rapid decrease of the F_v/F_m ratio with increasing irradiation time and light intensity (Supplemental Fig. S4). Wild-type leaves and leaves of *ohp1-1* and *ohp1-2* mutant plants were exposed to actinic illumination at 1,000 μmol photons m^{-2} s^{-1} and subsequently allowed to rest in darkness. Despite the fact that thylakoid membranes formed in pale-green leaves of *ohp1-1* and *ohp1-2* mutants, the time course of fluorescence measurements indicated large impairment of the mutants' photosynthetic functions (Supplemental Fig. S4A). F_v/F_m in wild-type plants decreased gradually as a result of photoinhibition, but F_v/F_m in the *ohp1-1* and *ohp1-2* mutants increased rapidly at a relatively low light intensity (Supplemental Fig. S4B).

The quantum yield of PSII electron transport also decreased in *ohp1-1* and *ohp1-2* mutants, as reflected in the suppressed growth of the plants. Nonphotochemical quenching (NPQ), a reflection of the plant's ability to dissipate excess light energy as heat (Müller et al., 2001), supported the above-mentioned results. In wild-type plants, NPQ increased greatly in plants grown under low light compared with plants grown under high light intensity (Supplemental Table S1). In contrast, NPQ of *ohp1-1* and *ohp1-2* mutants remained low even under low-light growth conditions. Accordingly, the qL parameter was higher in the mutants (Supplemental Table S1). qL is considered to be a better parameter than qP to estimate the redox state of the Q_A electron acceptor of PSII (Kramer et al., 2004); it indicates a more oxidized plastoquinone pool in the mutants. Taken together, chlorophyll fluorescence analyses suggested that the *ohp1* mutation affected PSII function.

PSII Complexes Are Impaired in *ohp1* Mutants

To study the accumulation of photosynthetic complexes in *ohp1* mutants, we extracted total proteins from leaf discs prepared from wild-type, *ohp1-1*, *ohp1-2*, and four *ohp1*-complemented plants and, after extraction with a mild detergent, dodecyl-α-D-maltoside (α-DM; Supplemental Fig. S5A) or dodecyl-β-D-maltoside (β-DM; Supplemental Fig. S5B), analyzed the protein complexes using blue native PAGE (BN-PAGE). In both BN gels and gels stained with Coomassie Brilliant Blue, protein complexes extracted from complemented *ohp1* plants that produced OHP1-epitope tag fusion proteins migrated in a pattern similar to that of wild-type plants. Complemented *ohp1-1* had fewer PSII monomers, possibly because of more robust supercomplex accumulation. However, the two *ohp1* mutants showed different patterns for the PSII protein complexes (Supplemental Fig. S5). LHCII trimers were detected at high levels in all accessions, but little or no other pigment-protein complexes were detected. Weak bands were visible in the mutants at positions where monomeric PSI and the PSII dimer comigrate. It is likely that dimeric PSII is absent and only monomeric PSI remains at this position, considering that PSII supercomplexes and monomeric PSII were absent in the *ohp1* mutants. Taken together, these results indicate that OHP1 is necessary for the accumulation of PSII complexes.

We analyzed photosynthetic protein contents of *ohp1* mutants and wild-type plants by immunoblotting (Fig. 3). Based on equal amounts of chlorophyll from wild-type and mutant proteins. Different chlorophyll-binding proteins were not equally affected in the *ohp1* mutants: levels of chloroplast-encoded, chlorophyll *a*-binding PSII core proteins (PsbA, PsbB, PsbC, and PsbD) were below the limit of detection in the mutants, while PSI core proteins and antennae were reduced to a lesser extent (Fig. 3, right). Most of the LHCII proteins accumulated normally, but interestingly, Lhcb2 levels

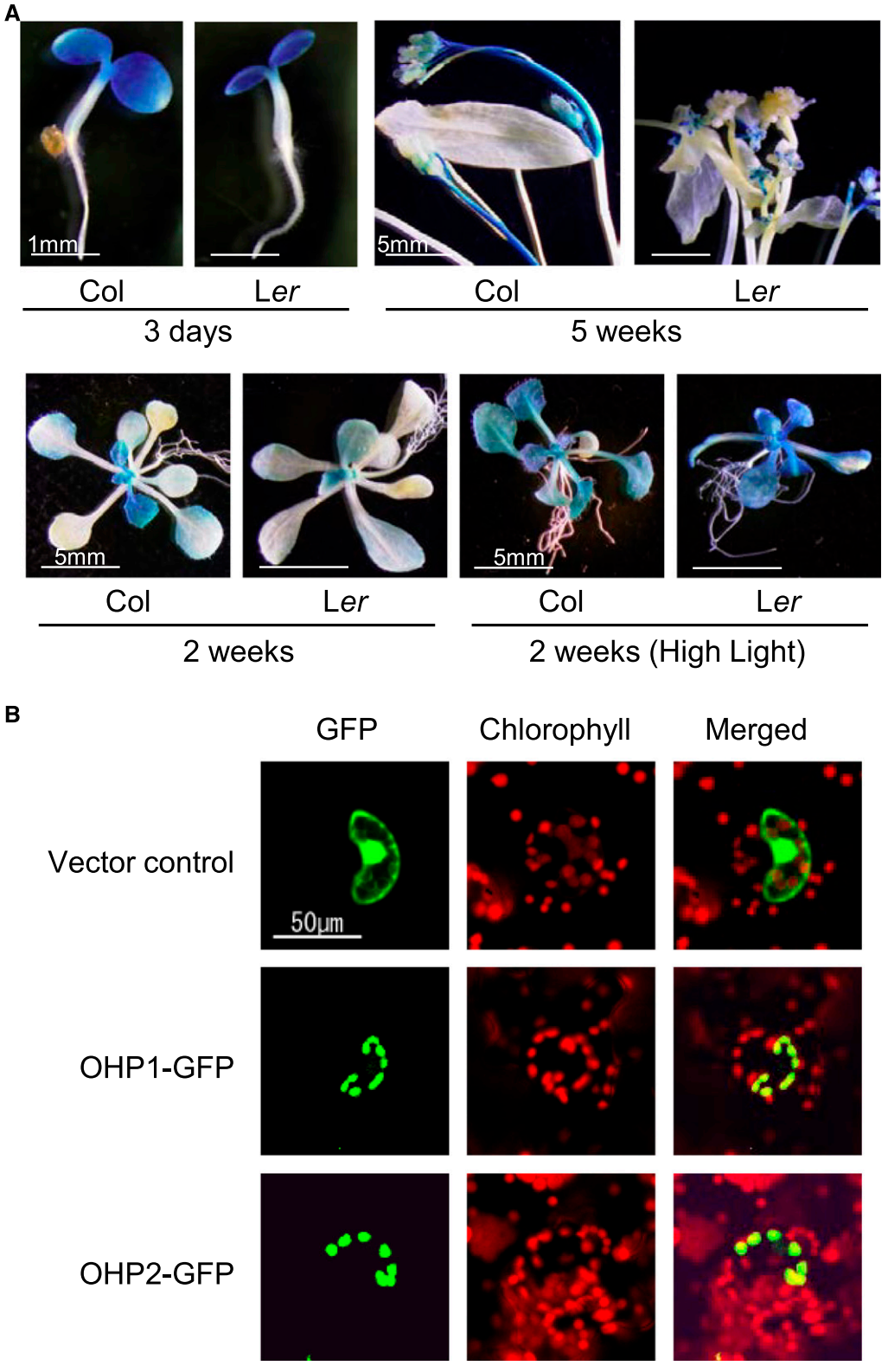

Figure 2. Histochemical analysis of *OHP1* expression and plastid targeting of chimeric sGFP protein. A, *GUS* expression patterns of transgenic Arabidopsis plants from Columbia (Col) and L*er* ecotypes harboring the OHP1 promoter plus the GUS reporter construct at different developmental stages: young seedlings 3 d after germination, bolting plants 2 weeks after germination, and flowering plants 5 weeks after germination. Transgenic plants were grown under unstressed conditions or under high-light treatment at 1,000 μmol photons m^{-2} s^{-1} for 1 h. Bars = 1 mm (young seedlings) or 5 mm (all other images). B, Plastid targeting of

were higher in the mutants. It is evident that the depletion of OHP1 severely affects the accumulation of the PSII core subunits, which likely led to the alteration of other subunits of photosystems, including CP1 and Lhcb2, although the control mechanisms of individual subunits are not yet clear.

Mutants lacking both Lil3.1 and Lil3.2 proteins are deficient in chlorophyll and accumulate unusual chlorophyll derivatives with incompletely reduced side chains (Tanaka et al., 2010; Lohscheider et al., 2015). Thus, we investigated the metabolic profiling of *ohp1* mutants but could not detect unusual chlorophyll derivatives (Supplemental Table S2). However, relative to the content of chlorophyll *a*, most pigments other than β-carotene increased in *ohp1* mutants compared with wild-type plants, indicating a decrease of relative chlorophyll *a* contents in *ohp1* mutants. These results were consistent with the aforementioned lack of obvious chlorophyll *a*-binding PSII core proteins in *ohp1* mutants (Fig. 3).

Association of OHP1 with Protein Complexes of Thylakoid Membranes

Thylakoid membranes were isolated from *ohp1-1* mutant plants that produced OHP1 with a C-terminal 3× hemagglutinin tag (OHP1-3xHA) or OHP1 protein with a C-terminal 10× Myc tag (OHP1-10xMyc) construct under the control of the *ohp1* native promoter (pOHP1::OHP1-HA and pOHP1::OHP1-Myc). The OHP1-3xHA fusions can completely complement the pale-green phenotype of the *ohp1* mutant, indicating that the tagged OHP1 protein is fully functional. However, the OHP1-10xMyc fusion construct could only partially complement the *ohp1* mutant phenotype, possibly because the long epitope tag compromised the function of OHP1. To analyze the composition of OHP1-containing complexes, we performed 2D BN/SDS-PAGE (two-dimensional BN-PAGE followed by SDS-PAGE) experiments to analyze thylakoid proteins prepared from *ohp1* plants that produced OHP1-Myc fusion proteins. While transgenic plants that produced OHP1-3xHA fusions presumably assemble OHP1 in PSII complexes similar to wild-type plants, the amount of OHP1 was below the immunological detection limit. Therefore, transgenic plants that produced the OHP1-10xMyc fusions were used for 2D BN/SDS-PAGE analysis. Several ionic detergents, such as α-DM, β-DM, and digitonin, were used to solubilize the thylakoid proteins. In pOHP1::OHP1-Myc in the *ohp1-1* mutant background, OHP1-Myc fusion proteins were always detected with masses of ~25, ~50, ~100, and ~200 kD (Fig. 4A), wherein the ~25-kD protein represented monomeric forms (OHP1-10xMyc; 24 kD) in the BN/SDS-PAGE. Immunoblotting analysis of wild-type thylakoid membranes after BN-PAGE analysis did not result in any signal (Supplemental Fig. S6A), indicating that immunostaining of the transgenic plants comes from OHP1-Myc fusion proteins. When another allele (*ohp1-2*) was used as a control, protein signals similar to those for OHP1-Myc were detected (Supplemental Fig. S6B). When thylakoid membranes were solubilized using β-DM, only two LHCII trimers were shown to bind strongly the core C_2S_2 PSII-LHCII supercomplex, in agreement with observations by Kouřil et al. (2012). However, when they were solubilized using α-DM, the PSII-LHCII supercomplexes were largely recovered as $C_2S_2M_2$-type supercomplexes, where two moderately bound LHCII trimers were additionally associated with C_2S_2-type supercomplexes (Ruban et al., 2003; Caffarri et al., 2009). When the thylakoid membrane was solubilized using 1% (w/v) digitonin, a nonionic detergent that is milder than α- and β-DM, somewhat different thylakoid protein complexes from those solubilized with α- and β-DM were detected, and signals of OHP1 were detected in larger protein complexes (Fig. 4A, bottom).

To further analyze the localization of OHP1, complexes from thylakoid proteins separated by 2D isoelectric focusing SDS-PAGE (i.e. isoelectric focusing separation followed by SDS-PAGE) were immunostained with representative antibodies directed against the epitope tag (Fig. 4A). Isoelectric focusing combines the use of an electric field with a pH gradient to separate proteins according to their pI. The pI values of OHP1 were predicted at pH 4; however, OHP1 was detected at more basic pH (Fig. 4, B and C), suggesting the formation of OHP1 complexes with additional protein components. On the other hand, the additional bands present in Figure 4, B and C, may just represent monomers that differ in charge due to posttranslational modification.

HCF244 Was Identified as a Partner That Interacts with OHP1

To identify proteins that interact with OHP1 in the PSII complex, we constructed transgenic lines (p35S:OHP1-FLAG/WT) in the L*er* background that produced OHP1 under the control of the CaMV 35S promoter with a 3xFLAG tag encoded at the C terminus of OHP1 in the wild-type L*er* background. The resulting p35S:OHP1-FLAG transgenic lines exhibited wild-type pigmentation (Supplemental Fig. S2B) and the presence of thylakoid membrane proteins identical to wild-type plants (Supplemental Fig. S7), indicating that

Figure 2. (*Continued.*)
the OHP1-sGFP chimeric protein in tobacco epidermal cells. Constructs carrying the control vector p35S-sGFP (top row), full-length OHP1-sGFP (middle row), and full-length OHP2-sGFP (bottom row) were bombarded into tobacco epidermal cells. Fluorescence from GFP (left) and chlorophyll autofluorescence (middle) was detected using a laser confocal-scanning microscope. At right, the two fluorescence images are merged. Bar = 50 μm.

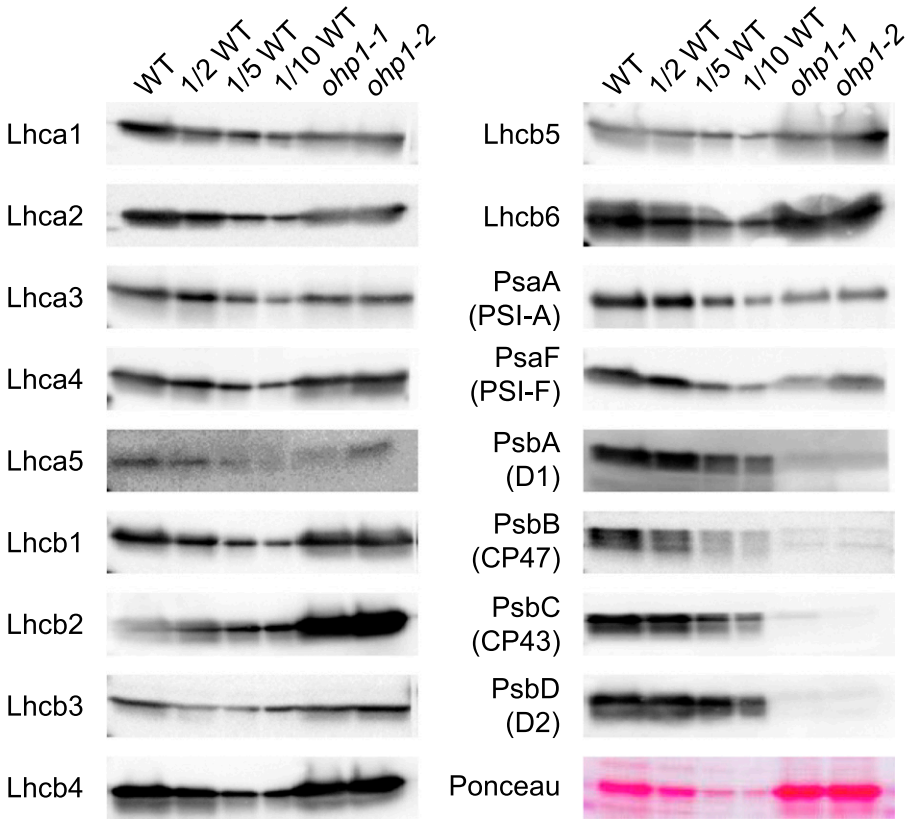

Figure 3. PSI- and PSII-related protein levels in *ohp1* mutants. The accumulation of photosynthetic proteins in the wild type (WT) and two alleles of the *ohp1* mutant (*ohp1-1* and *ohp1-2*) was studied through immunoblotting with monospecific antibodies labeled at the left side of the membranes. Lanes were loaded on the basis of 10 μg of chlorophyll per lane. Three dilutions of the wild type and two alleles of *ohp1* are shown, ordered according to their chlorophyll content (on a scale of 1 to 1/10, 1 being the highest). A fraction of a Ponceau S stain for the detection of proteins on nitrocellulose membranes shows the amount of thylakoid protein present in each lane.

FLAG-tagged OHP1 did not compromise the function of endogenous OHP1 protein. Thylakoid membranes were solubilized with 1% (w/v) α-DM or digitonin, and the resulting extract was applied to an anti-FLAG affinity column. Following extensive washing, the eluted material was separated by means of SDS-PAGE (Fig. 5A; Supplemental Fig. S8) and BN-PAGE (Fig. 5B). Gels stained by silver nitrates were digested with trypsin and identified by mass spectrometry (MS). In addition to the OHP1-FLAG protein used as bait (Fig. 5A; Supplemental Fig. S8, bottom band), we identified High Chlorophyll Fluorescence244 (HCF244 [At4g35250]; a putative homolog of cyanobacterial Ycf39) and OHP2 from two major protein bands (ii and v; Supplemental Fig. S8) by SDS-PAGE analysis of thylakoid proteins solubilized with 1% (w/v) α-DM (Table I; Supplemental Table S3). These two proteins, as well as HCF173 (At1g16720; a paralog of HCF244), HCF136 (At5g23120; a putative homolog of cyanobacterial Ycf48), and D1/D2 core proteins of PSII, were included in two complexes (I and II; Fig. 5B) obtained using BN-PAGE analysis of thylakoid proteins solubilized with 1% (w/v) digitonin (Table II; Supplemental Table S4). These proteins were not observed in samples extracted from the gel containing the control wild-type pull down. Furthermore, cytochrome b_{559} subunit α PsbE, ACCLIMATION OF PHOTOSYNTHESIS TO THE ENVIRONMENT1 (APE1), and LOW QUANTUM YIELD OF PSII1 (LQY1) were detected only in the larger complex I (Table II). To confirm the association of OHP1 with HCF244, we produced their epitope tag fusion proteins using a cell-free protein synthesis system from wheat germ (Supplemental Fig. S9) and performed in vitro protein-protein interaction assays based on amplified luminescent proximity homogenous assay technology (AlphaScreen technology; Perkin-Elmer). We observed concentration-dependent protein-protein interactions between biotinylated HCF244-His and OHP1-FLAG and between HCF244-FLAG and biotinylated OHP1-His (Fig. 5C). Interactions were significantly stronger than in the negative control, which lacked a vector. These observations suggest complex formation of OHP1-OHP2-HCF244-HCF136-HCF173 and the core components of PSII to form the assembly of the minimal reaction center complex of PSII.

DISCUSSION

The synthesis and assembly of the photosynthetic apparatus in plants are complicated processes that require coordinated expression of chloroplast- and nucleus-encoded genes and a large number of synthesis and assembly factors. An important step in the assembly of photosystems is the insertion of chlorophyll molecules into folding polypeptide chains of PSII, but the underlying mechanisms are unknown. This study provides evidence that two one-helix proteins (OHP1 and OHP2) are important for the assembly of pigment

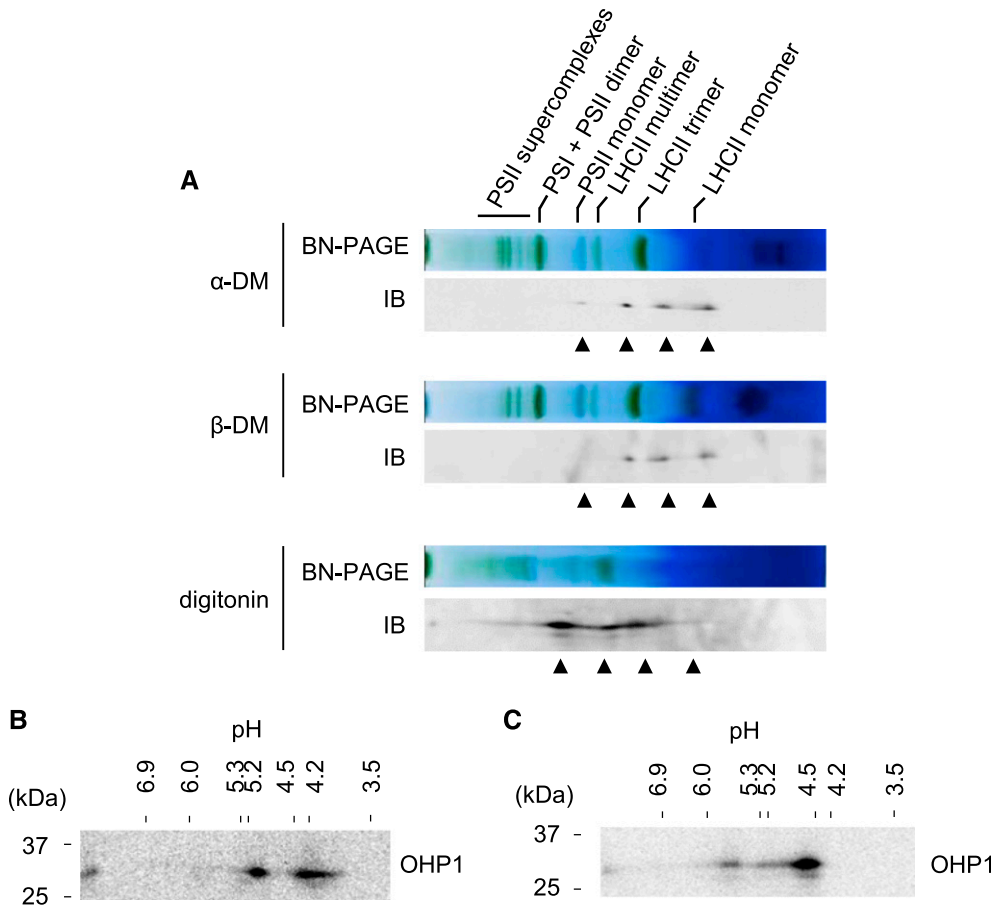

Figure 4. Different forms/complexes of OHP1 separated using BN/SDS-PAGE and 2D isoelectric focusing/SDS-PAGE. A, Thylakoid proteins in pOHP1::OHP1-Myc/*ohp1-1* corresponding to 7.5 μg of chlorophyll were solubilized for 30 min with 0.8% (w/v) α-DM (top), 0.8% (w/v) β-DM (middle), or 1% (w/v) digitonin (bottom) and then fractionated by BN-PAGE in the first dimension and by SDS-PAGE in the second dimension, followed by immunoblotting (IB) analysis using antibodies raised against OHP1-Myc proteins. The positions of the PSII-LHC supercomplexes and their derivatives indicated at the top of the BN gel are based on the analyses by Järvi et al. (2011), Takabayashi et al. (2011), and Takahashi et al. (2014). OHP1-Myc signals are indicated by the black arrowheads (molecular masses of ~25, ~50, ~100, and ~200 kD from the right side). B, Separation of distinct OHP1-Myc forms/complexes using 2D isoelectric focusing/SDS-PAGE after proteins were solubilized with α-DM. C, Separation of distinct OHP1-Myc forms/complexes using 2D isoelectric focusing/SDS-PAGE after proteins were solubilized with β-DM.

proteins. We identified Arabidopsis T-DNA-tagged mutant lines of *OHP1* and *OHP2* and observed remarkable defects in growth and photosynthesis in these mutants (Fig. 1; Supplemental Fig. S1). These results suggest that the two OHP proteins, OHP1/LIL2 and OHP2/LIL6, are essential for plant survival under normal growth conditions; mutant plants had pale-green leaves, showed severely retarded growth on MSM supplemented with Suc (Fig. 1A; Supplemental Fig. S1), and did not grow at all in soil. Transmission electron microscopy of the chloroplast ultrastructure in developing leaves of *ohp1* and *ohp2* mutant plants grown on MSM agar plates showed that chloroplasts of homozygous *ohp1* and *ohp2* mutants contained fewer thylakoid membranes with granal stacks than in wild-type plants (Fig. 1C; Supplemental Fig. S1), indicating that *ohp1* and *ohp2* mutations affected chloroplast development. The photosynthetic capacity of *ohp1-1* and *ohp1-2* mutants also was decreased significantly (Supplemental Table S1).

Transgenic plants complemented with OHP1 grew normally, confirming that growth defects in both *ohp1-1* and *ohp1-2* were caused by mutation of *OHP1* (Supplemental Fig. S2A). GUS reporter activity in pOHP1::*GUS* transgenic Arabidopsis plants was histochemically localized during early stages of leaf development under normal growth conditions (Fig. 2A). Moreover, GUS activity increased when plants were exposed to stress caused by high light intensity (Fig. 2A), which indicates important roles of OHP1 in plant responses to this stress. OHP1 and OHP2 proteins were localized in chloroplasts (Fig. 2B), and OHP1 was shown to function in the accumulation of PSII complexes (Fig. 3). The levels of PSII proteins decreased markedly in *ohp1* mutants, whereas the levels of PSI proteins were less affected. In contrast, LHCII proteins

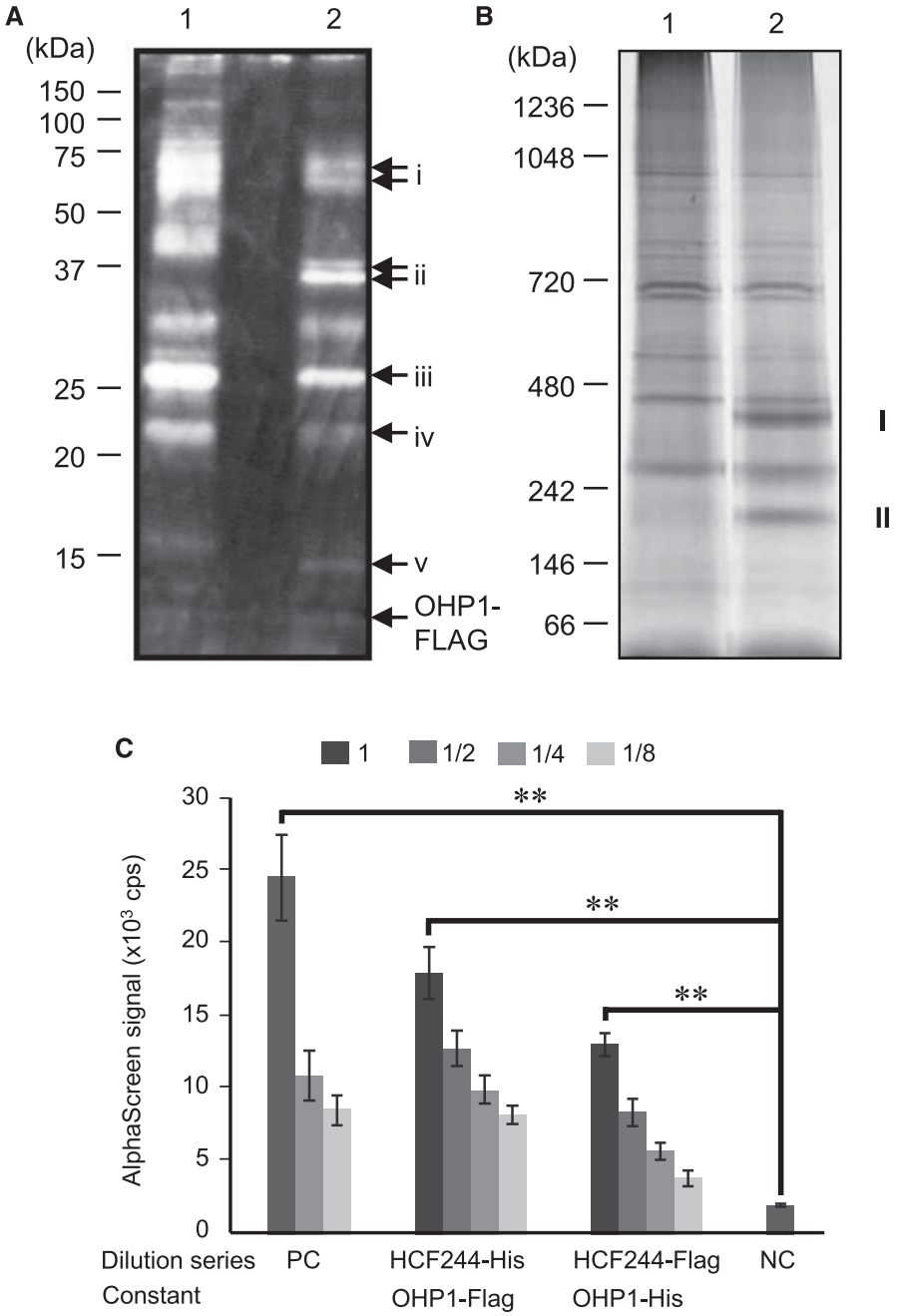

Figure 5. Identification of interacting protein partners of OHP1. A, Pull-down assay in wild-type plants (L*er* ecotype; lane 1) and the transgenic lines (p35S:OHP1-FLAG/WT L*er*; lane 2). The thylakoid membrane was solubilized with 1% (w/v) α-DM under native conditions on an anti-FLAG affinity gel. Eluted proteins were separated by SDS-PAGE and visualized with an Oriole stain. Designated protein bands (right side of gel, labeled i–v) were identified by means of MS (Table I; Supplemental Table S3). B, Eluted proteins from the thylakoid membrane of the transgenic line in A (lane 2) were solubilized with 1% (w/v) digitonin and separated by means of BN-PAGE together with a control pull down from the Arabidopsis wild-type plants (lane 1) and stained with silver salts. Two bands of large protein complexes (I and II) that differed from the wild type were analyzed by MS (Table II; Supplemental Table S4). C, AlphaScreening (amplified luminescent proximity homogenous assay) of protein-protein interactions. In vitro-synthesized OHP1 and HCF244 proteins were mixed with donor and acceptor beads, and detection of their luminescence was used to confirm their interaction. While OHP1 proteins remained constant, HCF244 proteins were diluted as indicated. Values represent the signal intensities of two independent experiments performed in triplicate (means ± SD). Significant differences compared with the negative control (NC): **, $P < 0.01$ (Student's one-tailed *t* test). PC, Positive control.

were produced at normal levels or overproduced in the *ohp1* mutants (Fig. 3). There is no doubt that the level of LHC protein decreased per individual leaf, as equal amounts of chlorophyll were loaded from the wild type and the mutants for analysis (the *ohp1* mutant exhibits a reduction of chlorophyll to ~40% of the wild-type level; Supplemental Fig. S2D). The striking difference in the levels of the PSII core subunits and LHC proteins clearly indicates that the mutation has greater impacts on the accumulation of the PSII core subunits. We speculate that the decrease in the LHCII level was, rather, a secondary effect of the decreased PSII core subunits in the *ohp1* mutants. Chlorophyll *a* and β-carotene were decreased severely in the *ohp1* mutant, which is consistent with the specific reduction of PSII core subunits (Supplemental Table S2). These results indicate that OHP1 plays a role in the de novo assembly of PSII, while *OHP1* also is induced in response to high-light stress.

Our study, together with a number of preceding studies, indicates that the machineries for PSII assembly are largely conserved between *Synechocystis* and Arabidopsis. Nonetheless, our data suggest that a diversity of partners that interact in PSII arose during the evolution of photosynthesis from cyanobacteria to plants. Compared with cyanobacteria, which have only one-helix members of the *Hlip/Scps* family as *Lil* genes in

Table I. *Proteins identified by means of liquid chromatography-tandem MS analysis from gel slices separated by means of SDS-PAGE after the OHP1-FLAG pull-down assay*

Band	Protein	Gene Name	Molecular Mass (D)	Coverage (%)
i	PTAC16, plastid transcriptionally active16	AT3G46780.1	54,359	32.9
	ATPB, ATP synthase subunit β	ATCG00480.1	53,935	43.8
ii[a]	HCF244, Arabidopsis homolog of the Ycf39 protein	AT4G35250.1	43,724	39.0
iii	Lhcb5, light-harvesting complex of PSII5	AT4G10340.1	30,158	21.4
iv	NPQ4/PsbS, chlorophyll *a*/*b*-binding family protein	AT1G44575.1	28,010	25.7
v[a]	OHP2, one-helix protein2	AT1G34000.1	18,666	40.1

[a]Two major protein bands for pull-down assay.

their genomes (Supplemental Fig. S10), plants contain a larger and more diverse family of LHC-related genes, which are called the LHC superfamily proteins, including LHC proteins, PsbS, and six LIL proteins. The *Synechocystis hliD/scpE* single-deletion mutant affected neither cell growth nor accumulation of the photosynthetic apparatus (Funk and Vermaas, 1999; He et al., 2001), despite a significant decrease in chlorophyll synthase levels and elevated accumulation of chlorophyllide (Chidgey et al., 2014), while a multiple deletion mutant of *Hlips* affected chlorophyll metabolism and C/N homeostasis (Xu et al., 2002; Tibiletti et al., 2016).

We used MS to identify proteins that coimmunoprecipitated with OHP1 and isolated HCF244, OHP2, HCF136, HCF173, and the PSII core protein (D1/D2) as binding partners of OHP1 (Table II). We confirmed the association of OHP1 with HCF244 by using a bead-based proximity assay for quantitative analysis (Fig. 5C). The *hcf244* mutants show the same phenotype as *ohp1* mutants (Link et al., 2012; Supplemental Fig. S11). Interestingly, the CP47-reaction center (RC47) complex in *Synechocystis* copurifies with Lil or the small CAB-like proteins ScpC and/or ScpD (Yao et al., 2007; Boehm et al., 2012). Recent studies reveal that cyanobacterial HliD/HliC binds to YidC, Ycf39, and chlorophyll synthase (Chidgey et al., 2014; Knoppová et al., 2014). Chloroplast Alb3, a homolog of bacterial YidC, associates with SecY translocase relatively weakly (Scotti et al., 2000; Klostermann et al., 2002), and core photosystem subunits are synthesized on Sec translocons associated with YidC/Alb3 (Sobotka, 2014). The Ycf39 homolog from Arabidopsis (HCF244) is involved in the translational initiation and stabilization of *PsbA* mRNA (Link et al., 2012), and cyanobacterial Ycf39 is speculated to be involved in the delivery of chlorophyll to newly synthesized D1 proteins and the stabilization of PSII reaction center complexes (Knoppová et al., 2014). Ycf39 and Ycf48 have similar functions in the de novo synthesis and assembly of the PSII complex. The *Synechocystis* Ycf48 protein is a component of an early PSII assembly complex and is important for both the efficient assembly of PSII by stabilization of a newly synthesized COOH-terminal precursor (pD1) and the selective replacement of photodamaged D1 during PSII repair (Komenda et al., 2008). OHP1 and OHP2 could have similar functions to HliD and HliC, respectively, and D1, D2, PsbE, and Ycf48 also were detected in association with the cyanobacterial HliD/HliC/Ycf39. Thus, OHP2, Ycf39/HCF244, Ycf48/HCF136, and the PSII core proteins D1/D2 were identified as common binding partners in *Synechocystis* and Arabidopsis, while HCF173, LQY1, and APE1 were identified as plant-specific binding partners of OHP1 (Fig. 5). HCF173, a distant homolog of HCF244, is involved in the translational initiation of the *psbA* mRNA in Arabidopsis (Schult et al., 2007; Link et al., 2012). Therefore, in cooperation with HCF244, HCF136, and HCF173,

Table II. *Complex I and II common and complex I-specific proteins identified by means of liquid chromatography-tandem MS analysis of two large protein complexes that were separated by means of BN-PAGE after the OHP1-FLAG pull-down assay*

Complex I and II common indicates proteins included in both complex I and II, and complex I specific indicates proteins included in complex I alone.

Protein Correlation Profiling	Protein	Gene Name	Molecular Mass (D)	Coverage (%)	
				I	II
Complex I and II common	HCF173, high chlorophyll fluorescence phenotype173	AT1G16720.1	65,710	14.4	1.5
	HCF136, PSII stability/assembly factor	AT5G23120.1	44,105	41.9	48.1
	HCF244, Arabidopsis homolog of Ycf39 protein	AT4G35250.1	43,724	40.5	53.2
	PsbD, PSII reaction center protein D	ATCG00270.1	39,549	22.7	9.1
	PsbA, PSII reaction center protein A	ATCG00020.1	38,938	31.4	3.1
	OHP2, one-helix protein2	AT1G34000.1	18,666	45.3	68.0
	OHP1, one-helix protein1	AT5G02120.1	12,011	35.5	35.5
Complex I specific	APE1, acclimation of photosynthesis to environment	AT5G38660.1	31,438	8.0	0
	LQY1, low quantum yield of PSII1	AT1G75690.1	16,334	28.6	0
	PsbE, PSII reaction center protein E	ATCG00580.1	9,397	22.9	0

OHP1 appears to associate with plastid-encoded PSII core subunits, and this is crucial for their assembly to form the PSII complex. Other proteins isolated with OHP1 also are involved in reaction center assembly or repair: PsbE is known as cytochrome b_{559} subunit α, LQY1 is involved in PSII repair (Lu et al., 2011; Jin et al., 2014), and APE1 is involved in photosynthetic acclimation to the light environment (Walters et al., 2003). According to our current working model of OHP1 (Fig. 6), OHP1-containing precomplexes, consisting of OHP1-OHP2-HCF244-HCF136-HCF173, are necessary to bind to the subunits of the PSII core complex that contains D1/D2 to form reaction center assembly complexes.

OHP1 is likely to be involved in more than the de novo synthesis of PSII reaction center complexes; it also appears to be involved in the repair of PSII after damage under stress conditions. We demonstrated that OHP1 is present in PSII at substoichiometric amounts; that is, the level of OHP1 is low in green leaves. However, OHP1 accumulates transiently during periods with high-light stress, which suggests that it may play a role in the protection of the PSII complex under these conditions (Supplemental Fig. S3B). According to current models in plants (Järvi et al., 2015), high light intensity and the resulting damage to the D1 protein lead to disassembly of the PSII dimer and phosphorylation of D1, D2, and CP43, which, in turn, triggers the migration of PSII to stroma-exposed regions of the thylakoid. Then, the PSII complex is dephosphorylated by PSII core phosphatase and partially disassembled by the release of CP43, which allows D1 degradation. Reorganization of the active PSII machinery is performed properly by assembly of the PSII complex with a newly produced active D1 protein in close association with assisting cofactors inside the complex. During the repair of PSII, damaged PSII complexes are transported to stroma-exposed regions of the thylakoid, where D1 is proteolytically degraded. Then, during the repair of PSII, ribosomes with *psbA* mRNA attach to D1-less PSII complexes and add the newly synthesized D1 protein to rebuild an active PSII complex. The ribosome appears to pause, awaiting chlorophyll insertion into the growing D1 protein. HliD, an OHP1 in the cyanobacterium *Synechocystis* sp. PCC 6803, binds specifically to chlorophyll *a* and β-carotene (Staleva et al., 2015). We hypothesize that the OHP1-HCF244 complex is involved in the delivery of chlorophyll *a* to the newly synthesized PSII core protein (D1/D2) during PSII repair.

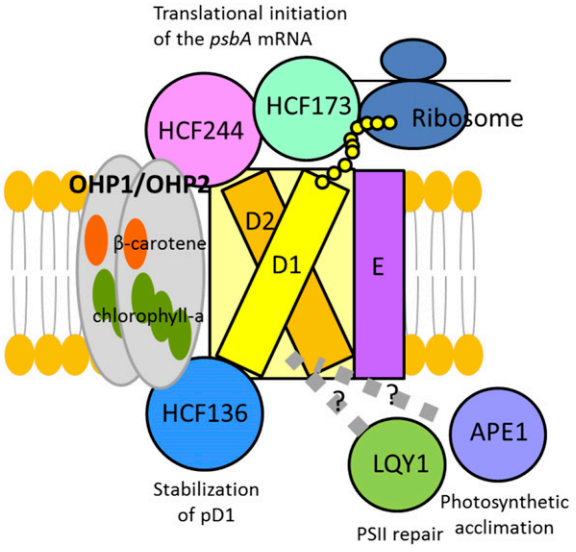

Figure 6. Schematic model for the role of OHP1-associated proteins during de novo assembly and repair of PSII. OHP1/OHP2 containing both chlorophyll *a* and β-carotene are in close contact with the D1/D2 reaction center of PSII. Chlorophyll *a* and β-carotene are incorporated via OHP1-HCF244/HCF173 into D1/D2 in the minimal reaction center complex that contains PsbE (E) but lacks CP47 and CP43. HCF244 and HCF173 act as RNA-binding proteins and facilitate the translation initiation of the *psbA* (D1) mRNA. Precursor D1 is synthesized and inserted into the membrane at a translocon-associated ribosome. HCF136 interacts with precursor D1 to form a D1 module, which binds to the D2 module and is involved in reaction center assembly. Other members isolated with OHP1 also are involved in reaction center assembly or repair: LQY1 is involved in PSII repair, and APE1 is involved in photosynthetic acclimatization to the light environment.

PSII complexes could not assemble in *ohp1* mutants, even when they were grown under dim light on agar plates supplemented with Suc, which suggests that PSII complexes in the mutants were vulnerable to light damage. In addition, PSII complexes in the mutants were able to perform charge separation and electron transport (Supplemental Table S1), which suggests the possibility that a small fraction of PSII spontaneously assembled in *ohp1* mutants under nutrient-sufficient conditions. We could not formally exclude the possibility that OHP1 is involved directly in thermal energy dissipation processes because of the diminished NPQ value in *ohp1* mutants (Supplemental Table S1). However, this effect is more likely a secondary consequence due to the absence of the core complexes. Also, the mobile antenna of PSII, which consists mainly of Lhcb1 and Lhcb2, was mostly unaffected in the *ohp1* mutant. The relatively high amounts of LHCII trimers and other LHC proteins in *ohp1* mutants suggest that the accumulation of LHC is regulated by an independent mechanism.

We hypothesize that OHP1 and OHP2 have distinct functions, as they do not functionally complement each other. Both single-knockout mutants showed an obvious chloroplast-defect phenotype, but the phenotypes were similar. We further demonstrated that OHP2 was one of the proteins that interacted strongly with OHP1, which indicates that these proteins work together rather than redundantly in the assembly of PSII complexes. OHP1 was localized around PSII (Fig. 5), and OHP2 has been shown previously to be an integral thylakoid membrane protein located within PSI. However, in the region of the detected PSI complexes, no probing of PSII presence was performed (Andersson et al., 2003). Our data do not exclude the possibility that the PSI complexes are in the same position as the PSII complexes. One possible explanation is that OHP2 was

present in PSII-containing supercomplexes comigrating with PSI by the dynamic movement of LHC that occurs during state transitions under certain light conditions. Whether the OHP1 complex also attaches to PSI remains unknown.

A recent report revealed that the loss of OHP1 and OHP2 leads to the loss of photosynthesis reaction centers and constant suffering from oxidative stress (Beck et al., 2017). These results also indicate that OHP1 and OHP2 are essential for functional photosynthesis in Arabidopsis. Phenotype analyses of two *ohp* mutants also showed their essential functions in photosynthesis. In this report, further functional analysis of OHP1 indicates that OHP1 forms a complex with PSII, which is important for its assembly and stabilization.

The report of Beck et al. (2017) and this study show that the *ohp1* and *ohp2* mutants may be grown on agar medium supplemented with Suc and develop pale-green leaves. The results of this study are the same as those of Beck et al. (2017) for the reduction of the PSII core complex. However, our finding that PSII efficiency, as measured by F_v/F_m ratios, is 0.5 or more in the *ohp1* and *ohp2* mutants indicates substantial residual PSII activity, whereas Beck et al. (2017) monitored a value close to zero. To the best of present knowledge, plants cannot grow when they completely lack PSII. It is most likely that the *ohp1* and *ohp2* mutants do accumulate a small amount of PSII, although no PSII was detected in the immunoblotting analysis. Given that the *ohp1* and *ohp2* mutants accumulate a small amount of PSII, it is not surprising that the F_v/F_m ratios are not zero. We think that the F_v/F_m values reported in this study better explain the phenotype of the *ohp1* and *ohp2* mutants.

In conclusion, the results of this study revealed that plants contain PSII assembly complexes similar to, but distinct from, the cyanobacterial counterpart. Cyanobacteria seem to have an alternative PSII assembly pathway that is not dependent on the OHP1 complex and that could be dependent on other factors (Nickelsen and Rengstl, 2013). In contrast, the OHP1 complex is indispensable for stable protein accumulation during the de novo synthesis of PSII in plants and is likely involved in the synthesis and assembly of the PSII machinery. This work is the first reported purification of the PSII reaction center complex that contains OHP1 in plants and will contribute to further dissection of the mechanism for PSII assembly in plants.

MATERIALS AND METHODS

Plant Materials and Growth Conditions

The pale-green *ohp1-1* and *ohp1-2* mutants were isolated from a large-scale collection of Arabidopsis (*Arabidopsis thaliana*) *Ds/Spm-* or T-DNA-tagged lines homozygous for nucleus-encoded chloroplast proteins by means of systematic phenotype analysis (Myouga et al., 2010, 2013), and the T-DNA was inserted into the first and second exons of At5g02120, respectively. We obtained T-DNA insertion lines GT_5_81048 (*ohp1-1*) from the European Arabidopsis Stock Centre (Sundaresan et al., 1995), GABI_362D02 (*ohp1-2*) and GABI_071E10 (*ohp2-2*) from the GABI-Kat (https://www.gabi-kat.de/) Arabidopsis collection (Rosso et al., 2003), and FLAG_016A10 (*ohp2-1*) from the Institut National de la Recherche Agronomique (Samson et al., 2002). The presence and locations of T-DNA insertions were confirmed in each mutant by means of PCR and sequence analysis. Wild-type and mutant seedlings were grown on MSM containing 1% Suc under long-day conditions (16 h of light/8 h of dark) with a photosynthetic photon flux density of 75 μmol m^{-2} s^{-1} at 22°C. Standard cloning techniques were used to develop the plant transformation constructs and generate transgenic plants. The multiple independent transgenic lines that produced each fusion protein reported in this study were T-DNA-homozygous plants in the F3 generation that were selected and tested by means of PCR and RNA gel-blot analysis to confirm high levels of transgene expression.

Vector Construction

Gateway recombination (Invitrogen) was used to generate vectors as described by Myouga et al. (2008). The genomic sequence, including promoter and coding regions of *OHP1*, was amplified from Columbia genomic DNA. The *OHP1* open reading frames were amplified from full-length cDNA clone RAFL06-08-F19, which is available from the RIKEN Bioresource Center. PCR was performed with high-fidelity PrimeSTAR HS DNA polymerase (Takara) in accordance with the manufacturer's recommended conditions. PCR fragments were cloned into the pDONR-D-TOPO entry vector (Invitrogen) and verified by sequencing. Entry clones were recombined into destination vectors using Gateway LR reactions with LR Clonase II (Invitrogen). For the complementation of mutant phenotypes, the genomic sequence of *OHP1* was cloned into several vectors (Nakagawa et al., 2007): pGWB4 (no promoter, C-sGFP), pGWB10 (no promoter, C-FLAG), pGWB13 (no promoter, C-3xHA), pGWB19 (no promoter, C-10xMyc), and pGWB22 (no promoter, C-GST). To overexpress *OHP1*, the *OHP1* open reading frame was cloned into the pGWB11 vector (35S promoter, C-FLAG) and the pGWB14 vector (35S promoter, C-3xHA). For histochemical analysis, the promoter sequence of *OHP1* was cloned into the pGWB3 vector (no promoter, C-GUS). To achieve transient expression in tobacco (*Nicotiana tabacum* 'SR1') leaves, the *OHP1* open reading frame was cloned into the pGWB5 vector (35S promoter, C-sGFP). After transfection in DH5α, stably transformed lines were cultured with appropriate antibiotics.

Transmission Electron Microscopy Observation

For transmission electron microscopy, samples were fixed with 2% glutaraldehyde and 4% paraformaldehyde in a 50 mM sodium cacodylate buffer, pH 7, at 4°C overnight and washed with the same buffer for 2 h at 4°C. They were then postfixed with 2% OsO_4 in a 50 mM sodium cacodylate buffer at 4°C for 2 h. Fixed samples were run through a series of increasing ethanol concentrations (up to 100%) and embedded in Spurr's resin. Ultra-thin sections (70 nm thick) were cut with a diamond knife on an Ultracut E ultra-microtome (Leica) and transferred to Formvar-coated grids. They were double stained with 1% (v/v) uranyl acetate for 20 min and with lead citrate solution for 15 min. After washing with distilled water, the samples were observed using a JEM-1200 EX transmission electron microscope (JEOL).

RNA Extraction, RT-PCR, and RNA Gel-Blot Analyses

Total RNA was isolated from 3-week-old Arabidopsis seedlings grown on MSM agar plates. RNA extraction, RT-PCR, and RNA gel-blot analyses were conducted as described by Myouga et al. (2006). For RT-PCR, the number of amplification cycles was reduced from 35 to 20 to evaluate and quantify any differences between transcript levels before the levels reached saturation. ACTIN2 (ACT2) and UBIQUITIN1 (UBQ1) were used as internal references. Gene-specific PCR products for *OHP1*, *OHP2*, *UBQ1*, and *ACT2* were obtained employing the following primers: OHP1_fw, 5′-CTACAAAGGAAAATAATGAGCTCG-3′; OHP1_rv, 5′-TAGAGGAAGATCGAGTCCTTT-3′; OHP2_fw, 5′-GCTTCGAAAATCAGACAATTCA-3′; OHP2_rv, 5′-TTCCAAGTCTAGAATGCCGAA-3′; UBQ1_fw, 5′-CGACAATGTCAAGGCCAAGA-3′; UBQ1_rv, 5′-TGGTTGCTGTGACCACACTT-3′; ACT2_fw, 5′-CTAAGCTCTCAAGATCAAAGG-3′; and ACT2_rv, 5′-ACATTGCAAAGAGTTTCAAGGT-3′.

Microscopy Analysis

GUS staining was performed as reported (Myouga et al., 2008). Developing seedlings were observed using a Leica MZ APO or an Olympus BX60 light microscope equipped with differential interface contrast optics. Images were recorded with a VB-7000 digital camera (Keyence). The subcellular localization of several OHP fusion proteins was analyzed using GFP fluorescence.

A construct of OHP-GFP was transiently transformed in tobacco leaves by using particle bombardment as described by Myouga et al. (2006), and GFP fluorescence was observed by confocal laser scanning microscopy (LSM510 Meta; Zeiss). For transmission electron microscopy, images were obtained as described (Myouga et al., 2008).

Measurement of Photosynthetic Parameters and of Chlorophyll and Pigment Contents

Photosynthetic parameters were calculated from chlorophyll fluorescence data collected with a portable pulse-amplitude-modulation fluorometer (MINI-PAM; Walz) as described by Myouga et al. (2008). Chlorophyll content was assayed as described by Myouga et al. (2006). Pigments were extracted from the leaves by grinding the tissues in 95% acetone. The pigment compositions of leaves and complexes were then analyzed by matching the absorption spectra of individual pigments to the absorption spectrum of acetone extract by means of HPLC (Tanaka et al., 2010).

Preparation and Immunoblotting of Thylakoid Membranes

Thylakoids were prepared from 6- to 7-week-old dark-adapted plants and then homogenized in a blender containing homogenization buffer (330 mM D-sorbitol, 50 mM HEPES-KOH [pH 7.5], 1 mM $MgCl_2$, 1 mM $MnCl_2$, 2 mM EDTA [pH 8], 0.2% bovine serum albumin, and 2 mM sodium ascorbate). The homogenate was then filtered through a Miracloth sheet (Calbiochem), and the filtrate was centrifuged at 4,000*g* for 20 s. Pellets were resuspended in 1 mL of homogenization buffer and loaded onto a three-layer Percoll (GE Health Sciences) gradient (10%, 40%, and 80% [v/v]). The gradient was centrifuged at 8,000*g* for 10 min. Sediment at the interface between the 40% and 80% layers was isolated and diluted to 10% of the original concentration in homogenization buffer. After centrifugation at 4,000*g* for 5 min, the pellets were gently resuspended in 1 mL of homogenization buffer to suspend intact chloroplasts. For the preparation of thylakoid membranes when chloroplasts were sonicated after hypotonic shock in a hypotonic buffer (5 mM Tricine-NaOH [pH 7.8], 5 mM NaCl, and 1 mM $MgCl_2$), ultrasonication was carried out on ice with an Ultrasonics cell disruptor (UD-211; TOMY) for 10 s at 30% maximum output. Thylakoid membranes were separated from the soluble fraction by centrifugation at 20,000*g* for 30 min, and the pellets were resuspended in resuspension buffer (600 mM sorbitol, 40 mM HEPES-NaOH, pH 7.6, 10 mM $MgCl_2$, 5 mM EDTA-NaOH, pH 7.5, and 20 mM KCl) and adjusted to a concentration of 1 mg mL^{-1} chlorophyll as determined photometrically (Myouga et al., 2006). Loading samples for immunoblotting were obtained by solubilizing the thylakoids with the nonionic detergents α-DM, β-DM, and digitonin (Sigma-Aldrich). SDS-PAGE and immunoblotting were performed as described previously (Damkjaer et al., 2009). All primary antibodies for immunoblotting were purchased from Agrisera.

Gel Electrophoresis

One-dimensional BN-PAGE and 2D BN/SDS-PAGE were carried out as described by Leoni et al. (2013) with minor modifications. Solubilized thylakoid membranes were separated on a 1-mm-thick 4% to 16% BN-PAGE gradient (Invitrogen) at 4°C, and then excised BN-PAGE lanes were layered onto 1-mm-thick Any kD Mini-PROTEAN TGX gels (Bio-Rad). Isoelectric focusing electrophoresis was performed at native conditions on Novex isoelectric focusing pH3-7 gels (Invitrogen), which include 5% acrylamide, 2.6% bis-acrylamide, TEMED, APS, ultrapure water, and 2% ampholytes, using the XCell SureLock Mini-Cell (Invitrogen). During Isoelectric focusing, proteins migrated in an electric field at a constant 100 V for 1 h, a constant 200 V for 1 h, and finished with a constant 500 V for 30 min at 4°C. Proteins separated by pI were fixed for 30 min using fixing solution containing 12% TCA with 3.5% sulfosalicylic acid to remove carrier ampholytes from the gel. After staining with Coomassie Blue and destaining the isoelectric focusing gel, the desired lane (strip) cut from the gel was transferred to an SDS gel, and 2D SDS-PAGE was performed.

Anti-FLAG Pull Down and Protein Identification

For the identification of proteins that interact with OHP1, membranes were solubilized in 1% (w/v) α-DM or 1% (w/v) digitonin, and then the samples were loaded onto FLAG-conjugated FG beads (anti-FLAG M2 affinity antibody [Sigma-Aldrich] on FG beads [Tamagawa Seiki]) and incubated with gentle agitation for 120 min at 4°C. The beads were then washed several times until the green color was removed using wash buffer containing 10 mM MOPS-KOH (pH 7.6), 4 mM $MgCl_2$, and either 1% α-DM or 1% digitonin. The beads were incubated with elution buffer containing a DYKDDDDK peptide (0.8 mg mL^{-1} [w/v]) in wash buffer. The eluted proteins were collected and used for BN-PAGE and SDS-PAGE, and proteins were then detected using a silver staining kit (Invitrogen) according to the manufacturer's instructions. Proteins were identified as described previously (Matsui et al., 2014) with minor modifications as specified in Supplemental Materials and Methods S1. Based on the exclusive unique peptide count, the composition of the OHP1 complex was determined by comparison with a molecular mass ladder composed of proteins with known weights and elucidating which proteins had higher counts than others (Table I) as well as which proteins had high counts in the transgenic lines but not in wild-type (*Ler*) Arabidopsis (Table II).

Cell-Free Protein Synthesis and Detection of Protein-Protein Interactions

To produce an expression vector for the wheat germ cell-free system, the gene's open reading frame was amplified by PCR and the amplified fragment was subcloned into pEU-FLAG or pEU-His-bls (with a biotin ligase site) vector according to the manufacturer's instructions (CellFree Sciences). In vitro transcription and cell-free protein synthesis were performed as described by Takai and Endo (2010). For cell-free protein synthesis, the ENDEXT Wheat Germ Expression Kit (CellFree Sciences) was used according to the manufacturer's instructions for the bilayer translation method. Biotinylated His fusion proteins were produced by incubation with biotin ligase produced by a wheat germ cell-free protein synthesis kit. To confirm protein-protein interactions, we performed chemiluminescence assays using AlphaScreen technology with EnSpire Plate Readers (Perkin-Elmer) according to the manufacturer's instructions.

Accession Numbers

Sequence data from this article can be found in the Arabidopsis Genome Initiative data library (https://www.arabidopsis.org/) with the following locus identifiers: OHP1 (At5g02120), OHP2 (At1g34000), ELIP1 (At3g22840), ELIP2 (At4g14690), LIL3.1 (At4g17600), LIL3.2 (At5g47110), PsbS (At1g44575), HCF244 (At4g35250), HCF136 (At5g23120), HCF173 (At1g16720), PsbE (AtCg00580), LQY1 (At1g75690), APE1 (At5g38660), UBQ1 (At3g52590), and ACT2 (At3g18780).

Supplemental Data

The following supplemental materials are available.

Supplemental Figure S1. Transmission electron micrographs of plastids in wild-type plants.

Supplemental Figure S2. Characterization of the *ohp1* and *ohp2* mutants and of transgenic lines expressing *OHP1* driven by CaMV 35S or native promoters.

Supplemental Figure S3. Accumulation of *OHP1* transcripts induced by high light intensity.

Supplemental Figure S4. Reduction of F_v/F_m under high-light stress.

Supplemental Figure S5. Analysis of photosynthetic protein complexes in wild-type plants and *ohp1* mutants using separation of thylakoid membrane proteins by BN-PAGE and Coomassie Brilliant Blue staining.

Supplemental Figure S6. Characterization of complexes containing OHP1-Myc proteins by using 2D BN/SDS-PAGE.

Supplemental Figure S7. Analysis of photosynthetic protein complexes in wild-type plants and the transgenic lines by using separation of thylakoid membrane proteins by BN-PAGE and Coomassie Brilliant Blue staining.

Supplemental Figure S8. OHP1-FLAG pull-down assay.

Supplemental Figure S9. In vitro protein synthesis expressed in the wheat germ cell-free expression system.

Supplemental Figure S10. Alignment of Arabidopsis OHP1 and OHP2 proteins with the *Synechocystis* HliA to HliD proteins.

Supplemental Figure S11. Phenotype of the *hcf244* mutants.

Supplemental Table S1. Photosynthetic parameters of Arabidopsis wild-type accessions used as mutant backgrounds and single-knockout mutants of *Lil* genes treated with different light intensities.

Supplemental Table S2. Determination of chlorophyll and carotenoid pigment contents in *ohp1* mutants and wild-type plants by means of HPLC.

Supplemental Table S3. MS analyses of stained gel bands separated by means of SDS-PAGE after immunoprecipitation of OHP1-FLAG.

Supplemental Table S4. MS analyses of stained gel bands separated by means of BN-PAGE after immunoprecipitation of OHP1-FLAG.

Supplemental Materials and Methods S1. Methods used to identify proteins.

ACKNOWLEDGMENTS

We thank Masae Kouno and Ikuko Ishihara (RIKEN Center for Sustainable Resource Science) for their technical support in managing the plant growth facility and Dr. Bernd Weisshaar (Max Planck Institute for Plant Breeding Research) for providing T-DNA mutants generated under the GABI-Kat program. We also thank Dr. Masatomo Kobayashi of the RIKEN Bioresource Center for providing the RAFL cDNA clones.

Received December 18, 2017; accepted January 25, 2018; published February 1, 2018.

LITERATURE CITED

Adamska I, Roobol-Bóza M, Lindahl M, Andersson B (1999) Isolation of pigment-binding early light-inducible proteins from pea. Eur J Biochem **260:** 453–460

Andersson U, Heddad M, Adamska I (2003) Light stress-induced one-helix protein of the chlorophyll *a/b*-binding family associated with photosystem I. Plant Physiol **132:** 811–820

Beck J, Lohscheider JN, Albert S, Andersson U, Mendgen KW, Rojas-Stütz MC, Adamska I, Funck D (2017) Small one-helix proteins are essential for photosynthesis in Arabidopsis. Front Plant Sci **8:** 7

Boehm M, Yu J, Reisinger V, Beckova M, Eichacker LA, Schlodder E, Komenda J, Nixon PJ (2012) Subunit composition of CP43-less photosystem II complexes of Synechocystis sp. PCC 6803: implications for the assembly and repair of photosystem II. Philos Trans R Soc Lond B Biol Sci **367:** 3444–3454

Caffarri S, Kouril R, Kereïche S, Boekema EJ, Croce R (2009) Functional architecture of higher plant photosystem II supercomplexes. EMBO J **28:** 3052–3063

Casazza AP, Rossini S, Rosso MG, Soave C (2005) Mutational and expression analysis of ELIP1 and ELIP2 in Arabidopsis thaliana. Plant Mol Biol **58:** 41–51

Chidgey JW, Linhartová M, Komenda J, Jackson PJ, Dickman MJ, Canniffe DP, Koník P, Pilný J, Hunter CN, Sobotka R (2014) A cyanobacterial chlorophyll synthase-HliD complex associates with the Ycf39 protein and the YidC/Alb3 insertase. Plant Cell **26:** 1267–1279

Damkjaer JT, Kereïche S, Johnson MP, Kovacs L, Kiss AZ, Boekema EJ, Ruban AV, Horton P, Jansson S (2009) The photosystem II light-harvesting protein Lhcb3 affects the macrostructure of photosystem II and the rate of state transitions in *Arabidopsis*. Plant Cell **21:** 3245–3256

Dolganov NA, Bhaya D, Grossman AR (1995) Cyanobacterial protein with similarity to the chlorophyll *a/b* binding proteins of higher plants: evolution and regulation. Proc Natl Acad Sci USA **92:** 636–640

Engelken J, Brinkmann H, Adamska I (2010) Taxonomic distribution and origins of the extended LHC (light-harvesting complex) antenna protein superfamily. BMC Evol Biol **10:** 233

Funk C (2001) The PsbS protein: a Cab-protein with a function of its own. *In* EM Aro, B Andersson, eds, Advances in Photosynthesis: Regulation of Photosynthesis, Vol 11. Kluwer Academic Publishers, Dordrecht, The Netherlands, pp 453–467

Funk C, Vermaas W (1999) A cyanobacterial gene family coding for single-helix proteins resembling part of the light-harvesting proteins from higher plants. Biochemistry **38:** 9397–9404

He Q, Dolganov N, Bjorkman O, Grossman AR (2001) The high light-inducible polypeptides in Synechocystis PCC6803: expression and function in high light. J Biol Chem **276:** 306–314

Hernandez-Prieto MA, Tibiletti T, Abasova L, Kirilovsky D, Vass I, Funk C (2011) The small CAB-like proteins of the cyanobacterium Synechocystis sp. PCC 6803: their involvement in chlorophyll biogenesis for photosystem II. Biochim Biophys Acta **1807:** 1143–1151

Jansson S (2005) A protein family saga: from photoprotection to light-harvesting (and back?). *In* B Demmig-Adams, ed, Photoprotection, Photoinhibition, Gene Regulation, and Environment. Advances in Photosynthesis and Respiration, Vol 21. Springer, Dordrecht, The Netherlands, pp 145–153

Jansson S, Andersson J, Kim SJ, Jackowski G (2000) An Arabidopsis thaliana protein homologous to cyanobacterial high-light-inducible proteins. Plant Mol Biol **42:** 345–351

Järvi S, Suorsa M, Aro EM (2015) Photosystem II repair in plant chloroplasts: regulation, assisting proteins and shared components with photosystem II biogenesis. Biochim Biophys Acta **1847:** 900–909

Järvi S, Suorsa M, Paakkarinen V, Aro EM (2011) Optimized native gel systems for separation of thylakoid protein complexes: novel super- and mega-complexes. Biochem J **439:** 207–214

Jin H, Liu B, Luo L, Feng D, Wang P, Liu J, Da Q, He Y, Qi K, Wang J, et al (2014) HYPERSENSITIVE TO HIGH LIGHT1 interacts with LOW QUANTUM YIELD OF PHOTOSYSTEM II1 and functions in protection of photosystem II from photodamage in *Arabidopsis*. Plant Cell **26:** 1213–1229

Kitajima M, Butler WL (1975) Quenching of chlorophyll fluorescence and primary photochemistry in chloroplasts by dibromothymoquinone. Biochim Biophys Acta **376:** 105–115

Klimmek F, Sjödin A, Noutsos C, Leister D, Jansson S (2006) Abundantly and rarely expressed Lhc protein genes exhibit distinct regulation patterns in plants. Plant Physiol **140:** 793–804

Klostermann E, Droste Gen Helling I, Carde JP, Schünemann D (2002) The thylakoid membrane protein ALB3 associates with the cpSecY-translocase in Arabidopsis thaliana. Biochem J **368:** 777–781

Knoppová J, Sobotka R, Tichy M, Yu J, Konik P, Halada P, Nixon PJ, Komenda J (2014) Discovery of a chlorophyll binding protein complex involved in the early steps of photosystem II assembly in Synechocystis. Plant Cell **26:** 1200–1212

Komenda J, Nickelsen J, Tichý M, Prásil O, Eichacker LA, Nixon PJ (2008) The cyanobacterial homologue of HCF136/YCF48 is a component of an early photosystem II assembly complex and is important for both the efficient assembly and repair of photosystem II in Synechocystis sp. PCC 6803. J Biol Chem **283:** 22390–22399

Kouřil R, Dekker JP, Boekema EJ (2012) Supramolecular organization of photosystem II in green plants. Biochim Biophys Acta **1817:** 2–12

Kramer DM, Johnson G, Kiirats O, Edwards GE (2004) New fluorescence parameters for the determination of QA redox state and excitation energy fluxes. Photosynth Res **79:** 209–218

Leoni C, Pietrzykowska M, Kiss AZ, Suorsa M, Ceci LR, Aro EM, Jansson S (2013) Very rapid phosphorylation kinetics suggest a unique role for Lhcb2 during state transitions in Arabidopsis. Plant J **76:** 236–246

Link S, Engelmann K, Meierhoff K, Westhoff P (2012) The atypical short-chain dehydrogenases HCF173 and HCF244 are jointly involved in translational initiation of the psbA mRNA of Arabidopsis. Plant Physiol **160:** 2202–2218

Liu Z, Yan H, Wang K, Kuang T, Zhang J, Gui L, An X, Chang W (2004) Crystal structure of spinach major light-harvesting complex at 2.72 A resolution. Nature **428:** 287–292

Lohscheider JN, Rojas-Stütz MC, Rothbart M, Andersson U, Funck D, Mendgen K, Grimm B, Adamska I (2015) Altered levels of LIL3 isoforms in Arabidopsis lead to disturbed pigment-protein assembly and chlorophyll synthesis, chlorotic phenotype and impaired photosynthetic performance. Plant Cell Environ **38:** 2115–2127

Lu Y (2016) Identification and roles of photosystem II assembly, stability, and repair factors in Arabidopsis. Front Plant Sci **7:** 168

Lu Y, Hall DA, Last RL (2011) A small zinc finger thylakoid protein plays a role in maintenance of photosystem II in *Arabidopsis thaliana*. Plant Cell **23:** 1861–1875

Matsui H, Fujiwara M, Hamada S, Shimamoto K, Nomura Y, Nakagami H, Takahashi A, Hirochika H (2014) Plasma membrane localization is essential for *Oryza sativa* Pto-interacting protein 1a-mediated negative regulation of immune signaling in rice. Plant Physiol **166:** 327–336

Mishra Y, Jänkänpää HJ, Kiss AZ, Funk C, Schröder WP, Jansson S (2012) Arabidopsis plants grown in the field and climate chambers significantly differ in leaf morphology and photosystem components. BMC Plant Biol **12:** 6

Müller P, Li XP, Niyogi KK (2001) Non-photochemical quenching: a response to excess light energy. Plant Physiol **125:** 1558–1566

Myouga F, Akiyama K, Motohashi R, Kuromori T, Ito T, Iizumi H, Ryusui R, Sakurai T, Shinozaki K (2010) The Chloroplast Function Database: a large-scale collection of Arabidopsis *Ds/Spm*- or T-DNA-tagged homozygous lines for nuclear-encoded chloroplast proteins, and their systematic phenotype analysis. Plant J **61:** 529–542

Myouga F, Akiyama K, Tomonaga Y, Kato A, Sato Y, Kobayashi M, Nagata N, Sakurai T, Shinozaki K (2013) The Chloroplast Function Database II: a comprehensive collection of homozygous mutants and their phenotypic/genotypic traits for nuclear-encoded chloroplast proteins. Plant Cell Physiol **54:** e2

Myouga F, Hosoda C, Umezawa T, Iizumi H, Kuromori T, Motohashi R, Shono Y, Nagata N, Ikeuchi M, Shinozaki K (2008) A heterocomplex of iron superoxide dismutases defends chloroplast nucleoids against oxidative stress and is essential for chloroplast development in *Arabidopsis*. Plant Cell **20:** 3148–3162

Myouga F, Motohashi R, Kuromori T, Nagata N, Shinozaki K (2006) An Arabidopsis chloroplast-targeted Hsp101 homologue, APG6, has an essential role in chloroplast development as well as heat-stress response. Plant J **48:** 249–260

Nakagawa T, Kurose T, Hino T, Tanaka K, Kawamukai M, Niwa Y, Toyooka K, Matsuoka K, Jinbo T, Kimura T (2007) Development of series of Gateway binary vectors, pGWBs, for realizing efficient construction of fusion genes for plant transformation. J Biosci Bioeng **104:** 34–41

Neilson JA, Durnford DG (2010) Evolutionary distribution of light-harvesting complex-like proteins in photosynthetic eukaryotes. Genome **53:** 68–78

Nickelsen J, Rengstl B (2013) Photosystem II assembly: from cyanobacteria to plants. Annu Rev Plant Biol **64:** 609–635

Niyogi KK, Li XP, Rosenberg V, Jung HS (2005) Is PsbS the site of non-photochemical quenching in photosynthesis? J Exp Bot **56:** 375–382

Rossini S, Casazza AP, Engelmann EC, Havaux M, Jennings RC, Soave C (2006) Suppression of both ELIP1 and ELIP2 in Arabidopsis does not affect tolerance to photoinhibition and photooxidative stress. Plant Physiol **141:** 1264–1273

Rosso MG, Li Y, Strizhov N, Reiss B, Dekker K, Weisshaar B (2003) An Arabidopsis thaliana T-DNA mutagenized population (GABI-Kat) for flanking sequence tag-based reverse genetics. Plant Mol Biol **53:** 247–259

Ruban AV, Wentworth M, Yakushevska AE, Andersson J, Lee PJ, Keegstra W, Dekker JP, Boekema EJ, Jansson S, Horton P (2003) Plants lacking the main light-harvesting complex retain photosystem II macroorganization. Nature **421:** 648–652

Samson F, Brunaud V, Balzergue S, Dubreucq B, Lepiniec L, Pelletier G, Caboche M, Lecharny A (2002) FLAGdb/FST: a database of mapped flanking insertion sites (FSTs) of Arabidopsis thaliana T-DNA transformants. Nucleic Acids Res **30:** 94–97

Schult K, Meierhoff K, Paradies S, Töller T, Wolff P, Westhoff P (2007) The nuclear-encoded factor HCF173 is involved in the initiation of translation of the psbA mRNA in *Arabidopsis thaliana*. Plant Cell **19:** 1329–1346

Scotti PA, Urbanus ML, Brunner J, de Gier JW, von Heijne G, van der Does C, Driessen AJ, Oudega B, Luirink J (2000) YidC, the Escherichia coli homologue of mitochondrial Oxa1p, is a component of the Sec translocase. EMBO J **19:** 542–549

Sobotka R (2014) Making proteins green: biosynthesis of chlorophyll-binding proteins in cyanobacteria. Photosynth Res **119:** 223–232

Sobotka R, McLean S, Zuberova M, Hunter CN, Tichy M (2008) The C-terminal extension of ferrochelatase is critical for enzyme activity and for functioning of the tetrapyrrole pathway in Synechocystis strain PCC 6803. J Bacteriol **190:** 2086–2095

Staleva H, Komenda J, Shukla MK, Šlouf V, Kaňa R, Polívka T, Sobotka R (2015) Mechanism of photoprotection in the cyanobacterial ancestor of plant antenna proteins. Nat Chem Biol **11:** 287–291

Standfuss J, Terwisscha van Scheltinga AC, Lamborghini M, Kühlbrandt W (2005) Mechanisms of photoprotection and nonphotochemical quenching in pea light-harvesting complex at 2.5 A resolution. EMBO J **24:** 919–928

Stawski K, Banach M, Goc A (2014) Expression patterns of convergently overlapping Arabidopsis thaliana gene pairs OHP-NDP1 and OHP2-MES14. Acta Biol Cracov Bot **56:** 80–89

Storm P, Hernandez-Prieto MA, Eggink LL, Hoober JK, Funk C (2008) The small CAB-like proteins of Synechocystis sp. PCC 6803 bind chlorophyll: in vitro pigment reconstitution studies on one-helix light-harvesting-like proteins. Photosynth Res **98:** 479–488

Sundaresan V, Springer P, Volpe T, Haward S, Jones JD, Dean C, Ma H, Martienssen R (1995) Patterns of gene action in plant development revealed by enhancer trap and gene trap transposable elements. Genes Dev **9:** 1797–1810

Takabayashi A, Kurihara K, Kuwano M, Kasahara Y, Tanaka R, Tanaka A (2011) The oligomeric states of the photosystems and the light-harvesting complexes in the Chl b-less mutant. Plant Cell Physiol **52:** 2103–2114

Takahashi K, Takabayashi A, Tanaka A, Tanaka R (2014) Functional analysis of light-harvesting-like protein 3 (LIL3) and its light-harvesting chlorophyll-binding motif in Arabidopsis. J Biol Chem **289:** 987–999

Takai K, Endo Y (2010) The cell-free protein synthesis system from wheat germ. Methods Mol Biol **607:** 23–30

Tanaka R, Rothbart M, Oka S, Takabayashi A, Takahashi K, Shibata M, Myouga F, Motohashi R, Shinozaki K, Grimm B, et al (2010) LIL3, a light-harvesting-like protein, plays an essential role in chlorophyll and tocopherol biosynthesis. Proc Natl Acad Sci USA **107:** 16721–16725

Tibiletti T, Hernández-Prieto MA, Matthijs HC, Niyogi KK, Funk C (2016) Deletion of the gene family of small chlorophyll-binding proteins (ScpABCDE) offsets C/N homeostasis in Synechocystis PCC 6803. Biochim Biophys Acta **1857:** 396–407

Walters RG, Shephard F, Rogers JJ, Rolfe SA, Horton P (2003) Identification of mutants of Arabidopsis defective in acclimation of photosynthesis to the light environment. Plant Physiol **131:** 472–481

Xu H, Vavilin D, Funk C, Vermaas W (2002) Small Cab-like proteins regulating tetrapyrrole biosynthesis in the cyanobacterium Synechocystis sp. PCC 6803. Plant Mol Biol **49:** 149–160

Xu H, Vavilin D, Funk C, Vermaas W (2004) Multiple deletions of small Cab-like proteins in the cyanobacterium Synechocystis sp. PCC 6803: consequences for pigment biosynthesis and accumulation. J Biol Chem **279:** 27971–27979

Yao D, Kieselbach T, Komenda J, Promnares K, Prieto MA, Tichy M, Vermaas W, Funk C (2007) Localization of the small CAB-like proteins in photosystem II. J Biol Chem **282:** 267–276